Published in final edited form as:
Biochim Biophys Acta. 2009 July ; 1793(7): 1199–1209. doi:10.1016/j.bbamcr.2009.04.012.

Regulation of the formation and trafficking of vesicles from Golgi by PCH Family Proteins During Chemotaxis

S. Lee, **J. W. Han**, **L. Leeper**, **J. S. Gruver**, and **C. Y. Chung***
Department of Pharmacology, Vanderbilt University Medical Center, Nashville, TN 37232-6600

Abstract

Previous study demonstrated that WASP localizes on vesicles during *Dictyostelium* chemotaxis and these vesicles appear to be preferentially distributed at the leading and trailing edge of migrating cells. In this study, we have examined the role of PCH family proteins, Nwk/Bzz1p-like protein (NLP) and Syndapin-like protein (SLP), in the regulation of the formation and trafficking of WASP-vesicles during chemotaxis. NLP and SLP appear to be functionally redundant and deletion of both *nlp* and *slp* genes cause the loss of polararized F-actin organization and significant defects in chemotaxis. WASP and NLP are colocalized on vesicles and interactions between two molecules via the SH3 domain of NLP/SLP and the proline-rich repeats of WASP are required for vesicle formation from Golgi. Microtubules are required for polarized trafficking of these vesicles as vesicles showing high directed mobility are absent in cells treated with nocodazole. Our results suggest that interaction of WASP with NLP/SLP is required for the formation and trafficking of vesicles from Golgi to the membrane, which might play a central role in the establishment of cell polarity during chemotaxis.

Keywords

WASP; PCH family protein; Vesicle trafficking; Actin; Cytoskeleton; Cell Polarity

INTRODUCTION

Chemotaxis, directed movement towards a chemoattractant agent, is a fundamental process of many cell types and is involved in diverse biological responses, including: migration of leukocytes and macrophages to inflammation sites, metastasis of tumor cells, and aggregation leading to the formation of the multicellular organism in *Dictyostelium* [1–4]. During these processes, the actin cytoskeleton is dynamically changed, a process that involves F-actin polymerization and depolymerization and the reorganization of existing filament networks. The first step of chemotactic movement is a chemoattractant-mediated increase in F-actin polymerization at the leading edge of the cell, which provides the motive force for pseudopod extension and cell movement. The Wiskott-Aldrich Syndrome protein (WASP) and related proteins (N-WASP and SCAR/WAVE) have emerged as key downstream components converging on multiple signaling pathways to F-actin polymerization. The proline-rich segment of WASP interacts with a number of proteins containing SH3 domains, many of which are involved in the regulation of cytoskeletal structure[5,6]. One of the SH3 proteins known

Address correspondence to: Chang Y. Chung, 468 Robinson Research Building (MRB I), 1215 21st Ave. South @ Pierce, Nashville, TN 37232-6600; Phone: 615-322-4956; Fax: 615-343-6532; Email: E-mail: chang.chung@vanderbilt.edu.

to interact with WASP is Cdc42-interacting Protein 4 (CIP4), one of the pombe Cdc15 homology (PCH) family proteins.

The PCH family proteins are characterized by the presence of an evolutionarily conserved FER-CIP4 homology (FCH) domain and coiled coil (CC) region, and they induce tubular membrane invagination *in vivo* and deform liposomes into tubules in vitro [7–9]. They are also known as F-BAR-domain-containing proteins (F-BAR proteins) since the FCH and coiled-coil domains are structurally similar to Bin/amphiphysin/RVS (BAR) domains[10,11]. These two domains together were also called as the extended FC (EFC) domain[12]. Some PCH family members contain homology region 1 (HR1) domain, which interact with the Rho GTPases Cdc42, TC10, and Rnd2[13]. Most PCH proteins have one or more Src homology 3 (SH3) domains at the COOH terminus, binding to various target molecules, including dynamins, N-WASP, and formin [8,9,12,14,15]. Different members of the PCH family appear to regulate various aspects of actin organization. CIP4 binds to activated Cdc42 and, when overexpressed, decreases the number of stress fibers in fibroblasts [7]. Overexpression of rat synaptic, dynamin-associated protein I (Syndapin I) or Syndapin II, caused reorganization of cortical F-actin and formation of filopodia in HeLa cells [16]. PSTPIP2 is an actin bundling protein that stimulates formation of filopodia, inhibits ruffling and increases the motility of macrophages [17].

In a previous study, we demonstrated that actin cytoskeleton is highly polarized in chemotaxing *Dictyostelium* cells and that WASP, a major regulator of F-actin assembly, localizes on vesicles, and these vesicles appear to be preferentially distributed at the leading edge and uropod of chemotaxing cells[18]. In this study, we have examined the role of two PCH family proteins, NLP and SLP, in the regulation of the formation and trafficking of vesicles that are associated with WASP. NLP and SLP appear to be functionally redundant and the deletion of both NLP and SLP causes a loss of polarized F-actin organization and severe defects in chemotaxis. WASP and NLP/SLP are colocalized on vesicles, and interactions between SH3 domains of NLP/SLP and the proline-rich region of WASP are required for the formation and trafficking of these vesicles. Our results demonstrate that NLP/SLP play an essential role in controlling the formation and trafficking of WASP-associated vesicles.

MATERIALS AND METHODS

Molecular Biology

The full coding sequence of the *nlp* and *slp* cDNA were generated by PCR using a series of primers based on a sequence in The *Dictyostelium* Genome Project database (http://www.dictybase.org). PCR products were subcloned into the EcoRI–XhoI site of pSP72 and sequenced. A *nlp* knockout construct was made by inserting the blasticidin resistance cassette into a Bgl II site. A *slp* knockout construct was made by inserting hygromycin resistance cassette into a BamHI site created at nucleotide 465 of the *slp* cDNA. These constructs were used for a gene replacement in the KAx-3 parental strain. Randomly selected clones were screened for a gene disruption by PCR, which was then confirmed by Southern blot analysis and RT-PCR. To YFP- or GST-fusion protein expression, *nlp* and *slp* cDNAs were subcloned into EXP-4(+) or pGEX plasmids, respectively.

Immunostaining and F-actin staining

Immunostaining was performed as described in the previous study[19]. For colocalization studies, a series of images with varying vertical focus (typically 10 images with 0.2 μm distance) was taken and reconstituted with deconvolution using Metamorph software and analyzed with colocalization measurement application of the Metamorph. Both source images

were thresholded prior to performing the colocalization measurement and the area of overlap between the two probes was measured as the percentage of whole image.

For phalloidin staining, cells were starved in 12 mM sodium phosphate buffer (pH 6.2) for more than 5 h and fixed with 3.7% formaldehyde for 5 min. Cells were permeabilized with 0.5% Triton X-100, washed, and incubated with FITC or TRITC-labeled phalloidin (Sigma) in PBS containing 0.5% BSA and 0.05% Tween-20 for 1 h. Cells were washed in PBS containing 0.5% Tween-20. Images were captured with Roper Coolsnap camera and Metamorph software. For labeling barbed-ends, aggregation competent cells were permeabilized with 100mM PIPES pH 6.9, 1% Triton X-100, 4% PEG, 1mM EGTA, 1mM MgCl2, 3μM phalloidin for 3 min and 0.4μM Rhodamine-labeled actin in 1μM ATP solution was added. After 5 min staining, cells were washed 3 times with PIPES buffer and fixed with 3.7% paraformaldehyde.

Chemotaxis assay

Cells competent to chemotax toward cAMP (aggregation-competent cells) were obtained by pulsing cells in suspension for 5 h with 30 nM cAMP and plated on glass-bottomed microwell dishes. A micropipette filled with 100 μM cAMP was positioned to stimulate cells by using a micromanipulator and DIC images of migrating cells were taken in 6 sec intervals for 15 min and analyzed with Metamorph software (Universal Imaging Corp., Downingtown, PA). Chemotaxis index is defined as $CI\ (t) = \cos(\theta(t))$, where θ = the frame by frame angle of turn for each cell in our sample and the index presented in the paper is average value of indices over the experiment.

In vivo actin polymerization assay

F-actin was quantified from TRITC-phalloidin staining of Dictyostelium cells as described in the previous study [20]. Cells were pulsed with 30 nM cAMP at 6 min intervals for 5 hr. Cells were diluted to 1×10^7 cells/ml and shaken at 200 rpm with 2 mM caffeine for 20 min to synchronize the signaling of the cells. Cells were spun and resuspended with phosphate buffer (10 mM PO_4 buffer, pH 6.1, and 2 mM $MgSO_4$) at 5×10^7 cells/ml and stimulated with 100 μM cAMP. 500 μl of cells were taken at 5, 10, 20, 30, 50, and 80 second time points and mixed with actin buffer (20 mM KH_2PO_4, 10 mM PIPES, pH 6.8, 5 mM EGTA, 2 mM $MgCl_2$) containing 6% formaldehyde, 0.15% Triton X-100, 1μM TRITC phalloidin. Cells were fixed and stained for 1 hr and spun down at 14,000 rpm for 5 min in the microfuge. Pelleted cells were extracted with 1 ml of 100% methanol and fluorescence was measured (540ex/575em). To determine nonsaturable binding, 100 μM unlabeled phalloidin was included.

Vesicle formation reconstitution assay

Vesicle budding assay was done as described in previous studies [24,25].

Preparation of cytosol—*Dictyostelium* cells were pulsed with 50 nM cAMP at 6-min intervals for 5 hrs. Cells were then pelleted at 800 g for 5 min, and washed once in homogenization buffer containing 125 mM KCl, 25 mM Hepes, pH 7.4. The cells were resuspended in homogenization buffer followed by homogenization using a stainless steel ball bearing homogenizer. The homogenate was centrifuged for 30 min at 214,000 g to get the cytosol fraction.

Preparation of permeabilized Dictyostelium cells—Approximately 2×10^7 cells were plated on 100 mm Petri-dish. Cells were washed 3 times with ice-cold swelling buffer containing 10 mM Hepes, pH 7.2 and 15 mM KCl. After a 10 min incubation on ice, the swelling buffer was aspirated and replaced with 1 ml breaking buffer (10 mM Hepes, 90 mM KCl) after which the cells were broken by scraping with a rubber policeman and 1 stroke of

homogenization. The cells were centrifuged at 800 g for 5 min, washed in 1 ml of breaking buffer, and resuspended in 400 ml of breaking buffer.

Reconstitution assay—Reconstitution assays for vesicle budding was done in a final volume of 600 ml containing: 240 ml permeabilized cells, 240 ml cytosolic extract (360 mg protein), 2.5 mM $MgCl_2$, 0.5 mM $CaCl_2$, 110 mM KCl, 1 mM ATP, 0.02 mM GTP, 10 mM creatine phosphate, 80 mg/ml creatine phosphate kinase, and protease inhibitors. Incubations were at RT for 1 hr and then centrifuged at 800 g for 5 min. After centrifugation, supernatant was removed and centrifuged for 30 min at 214,000 g. Supernatant and pellet were collected and run on SDS-PAGE gel to determine the amount of comitin by western blot.

RESULTS

WASP is associated with vesicles derived from Golgi

Our previous study demonstrated that GFP-WASP is associated with vesicles enriched with $PI(4,5)P_2$ and the basic (B) domain plays a major role for the interaction with $PI(4,5)P_2$[18], compared to uniform distribution of GFP (Fig. 1A). This vesicular localization of GFP-WASP can be recapitulated with YFP-tagged basic (B) and GTPase-binding (GBD) domains of WASP (YFP-B-GBD). To identify the origin of the these WASP-vesicles, we first examined the possibility of WASP- or YFP-B-GBD-associated vesicles being endosomes by staining cells with FM 4-64, a membrane-impermient lipophilic dye that fluoresces only when associated with membranes, and the internalization of the dye was monitored by fluorescence microscopy after washing out the dye. Plasma membranes become fully stained within seconds, and fluorescence then gradually accumulates in endocytic vesicles appearing as small cytoplasmic puncta. We found that fluorescence from FM 4-64 labeled endocytic vesicles does not colocalize with YFP-B-GBD-bound vesicles, indicating that YFP-B-GBD-bound vesicles are not derived from the endocytic process (Fig. 1B). To further examine the origin of the YFP-B-GBD-bound vesicles, the localization of these vesicles was compared to immunostaining of comitin (a marker for Golgi and Golgi-derived vesicles[21]), GFP-HDEL(an ER-specific retrieval signal in *Dictyostelium*[22]), and golvesin-c-GFP (a marker for Golgi but not for Golgi-derived vesicles[23]). The lack of strong colocalization of YFP-B-GBD with GFP-HDEL and golvesin-c-GFP, but the robust colocalization with comitin suggests that the vesicles containing WASP are likely to be derived from the Golgi (Fig. 1C).

Polyproline repeats of WASP are required for vesicle formation

Number of vesicles associated with YFP-B-GBD was remarkably reduced in cells expressing very low level of WASP ($WASP^{TK}$). WASP expression in $WASP^{TK}$ cells is regulated transcriptionally by a tetracycline (Tet)-regulated promoter/transcription activator combination (Tet-Off TA; tTA). Thus, the level of WASP transcript is very low in the absence of the Tet-off TA transcription activator[18]. This result indicates that WASP, and presumably F-actin polymerization, is required for the formation of these vesicles (Fig. 1A). Interestingly, YFP-B-GBD localized to the perinuclear area of $WASP^{TK}$ cells, suggesting that it localizes to the organelle such as Golgi or ER. To determine the role of the specific region of WASP for vesicle formation, we examined the localization of GFP-WASP lacking the polyproline region (WASPΔPro) or the WH1 domain (WASPΔWH1) in $WASP^{TK}$ cells (Fig. 2A). GFP-WASPΔWH1 appeared to be localized to vesicles, indicating that WH1 and B domains are not required for vesicle formation. However, these cells lack polarity and these vesicles did not show biased distribution to the leading edge and uropod. In contrast, few vesicles labeled with GFP-WASPΔPro were found and GFP-WASPΔPro localize to perinuclear area, suggesting that the polyproline region of WASP is required for the vesicle formation. These cells are not polarized and cannot extend pseudopodia effectively as shown in phase contrast pictures shown in Figure 2A. The polyproline region of mammalian WASP binds a number of SH3 domain-

containing proteins[24] and mutations within this domain of human WASP result in a severe WAS phenotype, indicating that the polyproline region plays an important role in the regulation of WASP function. We reasoned that the polyproline region is important for the formation of WASP-vesicles presumably via interaction with another protein containing a SH3 domain.

Interaction of NLP/SLP with the polyproline region of WASP

To identify proteins interacting with the polyproline region of WASP, we took advantage of the availability of the complete *Dictyostelium* genome to identify genes encoding proteins containing SH3 domain(s). Bioinformatic analysis of the *Dictyostelium* genome revealed that it contains 15 open-reading frames (ORFs) encoding SH3 domain-containing proteins. Two ORFs among these genes encode proteins similar to mammalian PCH proteins, Nwk/Bzz1p, Syndapin, and Cdc42-interacting protein 4 (CIP4) (Fig. 2B). CIP4 was originally identified as a protein interacting with activated Cdc42 and WASP by a two-hybrid screen[7], and it has been shown that the WASP-CIP4 interaction is mediated by the binding of the SH3 domain of CIP4 to the proline-rich segment of WASP. We reasoned that these two PCH family proteins are good candidates for the proteins interacting with the polyproline region of WASP. Based on taxonomic analysis and a previous study described these two genes[25], we named these genes Nwk/Bzz1p-like-protein (nlp; gene id: DDB0168480) and Syndapin-like protein (slp; gene id:DDB0203245). As shown in Fig. 2B, both NLP and SLP have an NH2-terminal FCH domain and coiled-coil region, or F-BAR domain together. The central region of the protein (homology region 1; HR1) was shown to interact with Cdc42[7]. Two SH3 domains for NLP and one for SLP are found in the COOH-terminus. To examine interactions between NLP/SLP and WASP, we performed a pull-down assay. Recombinant NLP was expressed and purified as a GST fusion protein and this was used to pull-down GFP-WASP from *Dictyostelium* cell lysates (Fig. 2C). The interaction between WASP and NLP/SLP presumably occurs through the SH3 domain of NLP/SLP as the SH3 domain of SLP is sufficient for pulling down WASP from cell lysates. The direct interaction between GST-WASP and His-NLP was confirmed with the pull-down assay (Fig. 2D). The interaction between NLP/SLP and WASP was consistent with the colocalization of two proteins in chemotaxing cells. In polarized cells, WASP and NLP colocalize on vesicles as seen when CFP labeled WASP is coexpressed with YFP-labeled NLP or SLP (Fig 2E), reinforcing the idea that they interact and colocalize to the same vesicular compartments. Colocalization analysis revealed that more than 80% of fluorescence intensity of CFP-WASP overlaps with YFP-NLP and YFP-SLP. Examination of YFP-B-GBD, YFP-NLP, and YFP-SLP revealed that their localization changes dramatically between vegetative growth and the onset of multicelluar development after starvation. In vegetative *Dictyostelium* cells lacking the polarity and rapid motility, the localization of YFP-B-GBD, YFP-NLP is perinuclear while YFP-SLP showed tubular networks at the periphery of cells in addition to the perinuclear localization. Both NLP and SLP localize to vesicles that showed biased distribution at the leading edge and uropod in developmentally committed and polarized cells (Fig. 2F), suggesting that WASP-vescle formation might be necessary and regulated during the onset of development. To examine the role of NLP and SLP, cells lacking *nlp* or *slp* were created by homologous recombination using hygromycin- and blastcidin-resistance genes, which was confirmed by Southern blot and reverse transcription-PCR (not shown). These cells did not show significant defects in chemotaxis or development, suggesting the functional redundancy of NLP and SLP. We then created a *nlp/slp* double null mutant that manifests a series of defects in chemotaxis and F-actin regulation.

WASP and NLP/SLP are required for vesicle formation at Golgi

Recent studies have shown that FBP17, a PCH family protein, binds to dynamin-2 and to N-WASP[26], both of which play important roles in forming endocytic vesicles[27,28]. The possibility that endocytosis might be impaired in *nlp/slp* cells was examined by staining cells with FM 1-43X and the internalization of the dye was monitored by fluorescence microscopy

after washing out the dye. To provide a quantitative assessment of endocytosis, we measured fluorescence intensities of cells in images collected with epifluorescence microscopy after 2 min incubation with FM 1-43 followed by a 10 min delay to allow for endocytosis. As illustrated in Figure 3A, *nlp/slp*$^{-}$ cells are active in endocytosis, as evidenced by the accumulation of fluorescent vesicles in the cell cytoplasm, and no significant differences in endocytosis were apparent when compared with wild type (KAx3) cells. Moreover, we subsequently observed FM1-43 fluorescent labeling in the ER surrounding the nucleus in both wild-type and *nlp/slp*$^{-}$ cells, presumably by retrograde membrane traffic through the endosome and Golgi. These observations strongly suggest that the formation of endocytic vesicles is generally unaffected in *nlp/slp*$^{-}$ cells and that cells are still capable of other membrane fusion events. Examination of the localization of YFP-B-GBD in *nlp/slp*$^{-}$ cells revealed that the localization of YFP-B-GBD on vesicles was lost and most of YFP-B-GBD localized to tubular structures in *nlp/slp*$^{-}$ cells. Localization of YFP-B-GBD in pernuclear area was also significantly increased in these cells. Immunostainings revealed the colocalization of GFP-HDEL and GFP-c-golvesin with YFP-B-GBD was significantly increased in *nlp/slp*$^{-}$ cells, suggesting that YFP-B-GBD or YFP-WASP might be entrapped in ER-Golgi area due to the inability of *nlp/slp*$^{-}$ cells to form WASP-associated vesicles (Fig. 3B). These results suggest that YFP-B-GBD vesicles are likely to be vesicles derived from Golgi, consistent with the possible role of WASP and PCH protein in vesicle formation. Lack of either WASP or NLP/SLP might cause the defect in vesicle formation, leading to the entrapment of YFP-B-GBD or YFP-NLP(not shown) to ER-Golgi at perinuclear area.

To study the role of NLP/SLP and WASP for vesicle formation from Golgi, we employed an assay that reconstitutes the formation of these vesicles in a cell-free system using a combination of cytosol fraction prepared from cell lysate and permeabilized cells[29,30]. Vesicle formation in this cell-free assay has been reported to be ATP-, GTP-, and cytosol-dependent[31]. 1 μM GTPγS abolished vesicle formation after 30 min of preincubation (Fig. 4A), suggesting the role of small GTPase in this process. Vesicle formation was markedly reduced in the reconstitution of the cytosol and permeabilized cells from *nlp/slp*$^{-}$ cells. The reconstituion of cytosol and permeabilized WASP^{TK} cells also showed significant reduction of vesicle formation. These results suggest that WASP and NLP/SLP are required for vesicle formation from Golgi. Defect of vesicle formation in these cells was rescued up to the level of wild type cells by adding GST-NLP in the cytosol, but GST-NLP lacking the FCH domain (NLP FCH) failed to rescue, indicating that the FCH domain is required for vesicle formation. To test the role of cytosolic proteins in vesicle formation, cytosol fractions of *nlp/slp*$^{-}$ or WASP^{TK} cells were added back to permeabilized wild type cells to test vesicle formation activity (Fig. 4B). Vesicle formation with cytosols from *nlp/slp*- or WASP^{TK} cells was not as active as with cytosol from wild type cells. Reciprocal addition of wild type cytosol to permeabilized WASP^{TK} cells resulted in a significant improvement of vesicle formation over WASP^{TK} cells, but still not comparable to the level of wild type cells. These results indicate that both cytosolic proteins and permeabilized cells are necessary for efficient vesicle formation from Golgi.

Aberrant F-actin organization and chemotaxis of *nlp/slp*- cells

To examine any defect in F-actin organization in *nlp/slp*- cells, we stained for actin filaments of aggregation-competent WT and *nlp/slp*- cells using rhodamine-phalloidin staining. The actin cytoskeleton controls the overall structure of cells and is highly polarized in chemotaxing cells, with F-actin localized predominantly in the anterior leading edge and to a lesser degree in the cell's posterior [32–34]. Wild-type cells are well polarized and show localized F-actin assembly at the lamellipodia of the leading edge and, to a lesser degree, at the posterior cortical region of the retracting cell body (uropod) (Fig. 5A). *nlp/slp*- cells exhibited severe defects in F-actin organization as they exhibit neither a prominent F-actin-enriched lamellipod nor cell polarity. Cortical F-actin level appears to be uniformly low along the cell pheriphery, indicating

the lack of polarized F-actin at the cortex. Expression of NLP or 2 rescues this defect and restores polarized F-actin organization. Interestingly, the F-actin organization was fully rescued by NLP expression, but not by SLP as these cells showed rather unifirm F-actin polymerization along the cortical membrane and more filopodia. *nlp/slp*- cells were tested for *in vivo* actin polymerization responses to cAMP stimulation. Wild-type cells show a rapid and transient increase of F-actin assembly (~70–90% increase) by 5 seconds after cAMP stimulation (Fig. 5B), as previously described [20,35]. *nlp/slp*- cells showed a moderately lower level of F-actin assembly (60% of wild type cells) in unstimulated cells, which is consistent with lower cortical F-actin levels shown by phalloidin staining in Fig. 5A. *nlp/slp*- cells also exhibited a significantly reduced level of F-actin assembly upon cAMP stimulation. More importantly, as shown in Fig. 5C, *nlp/slp*- cells show a greatly decreased number of free barbed ends at the membrane cortex upon cAMP stimulation relative to wild-type cells. In aggregation-competent wild-type cells, the distribution of free barbed ends was polarized and, upon uniform cAMP stimulation, the number of barbed ends, stained with fluorescently labeled G-actin, increases about 100% (Figure 5C). In *nlp/slp*- cells, the number of free barbed ends appears to be greatly reduced and did not show any significant increase upon cAMP stimulation. In our previous study, $WASP^{TK}$ cells showed similar reduction of free barbed-ends upon cAMP stimulation[18]. Combined with the inability of *nlp/slp*- cells to form WASP-vesicles from Golgi, this result suggests that lack of NLP/SLP might cause the lack of WASP at the membrane cortex leading to lack of the formation of free barbed-ends and F-actin polymerization upon cAMP stimulation.

To test whether the changes in the actin cytoskeleton described above alter chemoattractant-induced cell migration, we employed a micropipette chemotaxis assay combined with time-lapse video microscopy (Fig. 6A). Wild-type cells are usually well polarized, move quickly and linearly toward the cAMP source, extend pseudopodia predominantly in the direction of the cAMP gradient, and produce very few random lateral or rear pseudopodia. The polarization and chemotaxis of *nlp/slp*- cells are significantly impaired compared to wild type cells. They are flattened and round as they are unable to establish polarity (Fig. 6A). Even though *nlp/slp*- cells are bigger and flatter than wild type cells, it is rare to find multi-nucleated cells (not shown), indicating cytokinesis is not impaired. In the presence of a chemoattractant, *nlp/slp*- cells appear to have difficulties developing a psuedopod in the direction of the chemoattractant gradient. Also, the cell body does not polarize, resulting in very slow movement with a higher angular deviation due to lack of persistent movement toward the gradient. Thus, they move at a speed of 2–3 μm/minute, a fourth as fast as wild-type cells (8–10 μm/min) and chemotaxis indices of *nlp/slp*- cells are significantly lower than those of wild type cells. Chemotaxis defects of *nlp/slp*- cells appear not to be resulted from a gross defect of gene expression since cAMP receptor 1 (cAR1) expression was not grossly affected (data not shown). The expression of YFP-NLP alone mostly rescues motility defects seen in the double knockout even though polarity of cells did not appear to be recovered completely.

Interaction of NLP/SLP with MT might be required for vesicle formation and transport

The distribution of YFP-B-GBD-vesicles is polarized such that the vesicles are concentrated at the leading and uropod of the cell, suggesting that active transport of vesicles via microtubules (MTs) might be involved in this process. To elucidate the role of MT in the polarized distribution of WASP-vesicles, we examined the distribution of YFP-B-GBD-vesicles in cells treated with nocodazole (Fig. 7A). In morphologically polarized, highly motile wild type cells, MTs are aligned in parallel toward the leading edge and uropod. The distribution of YFP-B-GBD-vesicles is also polarized. Many vesicles in the cell body are localized in a close proximity of microtubules. Interestingly, vesicles are more concentrated in the area where MTs do not extend substantially into the F-actin-enriched leading edge. Nocodazole treatment depolymerized most MTs as confirmed by immunostaining of α–tubulin. Both the

morphological and vesicle distribution polarities are significantly reduced in nocodazole-treated cells, suggesting MTs play an important role for polarized distribution of YFP-B-GBD vesicles. We attempted to track movements of these vesicles in cells by video microscopy. Tracking of vesicle movements showed that it moved in a stochastic manner and frequently reversed its direction (Fig. 7B). In wild type cells (mean vesicle velocity 0.125 μm/sec), video microscopy analysis of vesicle movement showed highly variable travel distances and brief periods of rapid directed movement leading to high speed (>0.25 μm/sec). This is not likely to be due to the cell body displacement (mean velocity 0.16 μm/sec). However, vesicles showing high mobility are absent in cells treated with nocodazole (mean velocity 0.076 μm/sec). Thus, the biased distribution of WASP-vesicles and high velocity movement of these vesicles were significantly reduced by treatment of cells with nocodazole, suggesting that trafficking of these vesicles requires MTs. The F-BAR proteins share a conserved N-terminal FCH and Bin-Amphiphysin-Rvs (F-BAR) domain[10] and the F-BAR domain has been reported to be responsible for the interaction of CIP4 and Rapostlin/FBP17/FNBP1 with MTs[36][37,38]. This suggests an intriguing possibility that NLP1-MT interaction might help formation of WASP-vesicle and that the binding of NLP/SLP positive vesicles to MTs facilitates the trafficking of vesicles. To examine the interaction of NLP or SLP with MTs, we performed in an *in vitro* MT-binding assay. Both GST-NLP and SLP bind to MT while GST control did not show any binding to MT(Fig. 7C). SLP appears to have a stronger affinity for MT and the deletion of FCH domain of NLP caused moderately reduced binding to MT, indicating that the FCH domain might not be essential for MT binding. To test the possibility that NLP/SLP might mediate the interaction of YFP-B-GBD vesicles with MTs, we then examined if YFP-B-GBD can be cosedimented with MTs in a sucrose gradient (Fig. 7D). Lysate of wild type cells expressing YFP-B-GBD was layered on top of 15–40% sucrose gradient and centrifuged. YFP-B-GBD comigrates with MTs in fractions near the bottom of sucrose gradient, presumably via the interaction of YFP-B-GBD vesicles and MTs. This interaction appears to be dependent upon the presence of NLPs as the comigration between YFP-B-GBD and MT is completely eliminated due to the absence of NLP/SLP in *nlp/slp*$^{-}$ cells.

DISCUSSION

Directional cell movement requires a defined cell polarity in which components of the cytoskeleton are differentially localized at the leading, front edge of a migrating cell [39]. Our previous study demonstrated that GFP-WASP are localized on vesicles that are preferentially distributed at the leading edge and uropod, suggesting that localization of WASP might control the polarized F-actin assembly during chemotaxis[18]. In this study, we demonstrated that the interaction between the polyproline repeats of WASP and the SH3 domain of NLP or SLP is required for the formation and trafficking of these vesicles to the cortical membrane as cells lacking WASP or NLP/SLP showed defects in vesicle formation and in organizing polarized F-actin at the membrane cortex.

NLP and SLP appears to be functionally redundant based on the lack of null phenotypes in single null mutant. YFP-NLP or YFP-SLP expressed in *nlp/slp*$^{-}$ null cells also showed similar change of the subcellular localization between vegetative growth and the onset of multicelluar development. In vegetative *Dictyostelium* cells lacking the polarity, the localization of YFP-NLP and SLP is perinuclear while NLP and SLP localizes to vesicles that showed biased distribution at the leading edge and uropod in polarized and chemotaxing cells. It is likely that formation and trafficking of these vesicles are induced by the differentiation of cells. However, we observed subtle functional differences between NLP and SLP. YFP-SLP showed tubular networks at the periphery of cells in addition to the perinuclear localization. In addition, F-actin organization defect of *nlp/slp*$^{-}$ null cell was fully rescued by the expression of NLP, but not SLP as these cells showed rather uniform F-actin polymerization along the cortical

membrane and more filopodia. It is likely that two SH3 domains of NLP might be required for full rescue of *nlp/slp*- null phenotype and more specific localization.

Studies have shown that actin is clearly involved in endocytic vesicle formation. The initial internalization of clathrin-coated vesicles is at least regulated by a family of proteins that interact with or modify the actin cytoskeleton[40,41]. FBP17 and/or CIP4, both members of the PCH protein family, have been shown to contribute to the formation of the protein complex, including N-WASP and dynamin-2, in the early stage of endocytosis, indicating that PCH protein family members couple membrane deformation to actin cytoskeleton reorganization in various cellular processes[12]. Recently, it has been shown that membrane endocytosis remains active in aggregation-competent *Dictyostelium* cells, and cells rapidly endocytose their plasma membrane in small vesicles, and return it to the surface within a few minutes[42]. Thus, one might imagine that *nlp/slp*- null cells would show defects in endocytosis. It was rather surprising that NLP and SLP appear not to play essential roles in endocytic processes as *nlp/slp*- cells showed no significant defects in endocytosis. The requirement for actin in vesicular trafficking from Golgi has been demonstrated in the study showing the inhibition of post-Golgi traffic of non-raft associated cargos with the actin-stabilizing jasplakinolide or the actin-depolymerizing latrunculin B[43]. It has been also reported that some vesicles of Golgi origin are propelled into the cytoplasm by actin polymerization[44–46] and actin regulation by Arp2/3 and Hip1R has been suggested to be necessary for the efficient release of clathrin-coated vesicles from the TGN[47]. Syndapin I, a member of PCH family proteins, has been reported to play an important role for vesicle formation from the Golgi and interaction of the syndapin SH3 domain with the proline-rich domain of dynamin II was reported to be critically important for vesicle formation[14]. Our findings are consistent with the role of PCH family protein in the formation of vesicles from the Golgi. Comitin, a marker of Golgi-derived vesicles, colocalized with NLP and WASP on vesicles, suggesting that WASP-associated-vesicles are likely to be exocytic vesicles derived from the Golgi. WASP and NLP/SLP are apparently involved in the formation of these vesicles as we demonstrated defects of $WASP^{TK}$ and *nlp/slp*- cells in vesicle budding from Golgi *in vivo* and *in vitro*. Colocalization of YFP-B-GBD with GFP-HDEL and Golvesin-c-GFP in *nlp/slp*- cells suggest that WASP might be trapped in the ER-Golgi where vesicle formation can't be completed due to the lack of NLP/SLP, causing lack of WASP trafficking to the cortex. Lack of barbed ends formation at the cortex upon cAMP stimulation in *nlp/slp*- cells is consistent with reduced WASP-vesicle formation and trafficking to the membrane cortex. Our previous study demonstrated that GFP-WASP- or YFP-B-GBD-associated vesicles can be labeled with CFP-tagged PH domain of PLCδ1, indicating that these vesicles are enriched with $PI(4,5)P_2$[18]. It is possible that $PI(4,5)P_2$ might recruit WASP and NLP/SLP to ER/Golgi membrane since WASP and PCH family proteins have been shown to interact with $PI(4,5)P_2$. Previous studies reported that the basic domain of WASP or N-WASP interacts with $PI(4,5)P_2$[48,49] and that the induction of actin polymerization resulted from the recruitment of N-WASP to PI(4,5)P2 vesicles. The extended FC (EFC) domain (FCH plus CC) of CIP4, and other PCH protein family members bind strongly to phosphatidylserine and PI(4,5)P2[12]. In this study, we demonstrated that the FCH domain of NLP is required for vesicle budding, consistent with the idea that the recruitment and formation of the protein complex, including CIP4 and WASP, on $PI(4,5)P_2$-enriched Golgi membrane might couple membrane deformation to actin cytoskeleton reorganization in vesicle formation. The crystal structures of the EFC domains of human FBP17 and CIP4 revealed a gently curved helical-bundle dimer which forms filaments through end-to-end interactions in the crystals, and the curved EFC filament is proposed to drive membrane tubulation[50]. One might imagine that PI(4,5)P2 has a regulatory role in the formation of this filament.

We demonstrated the binding of NLP and SLP to MT and the loss of polarized distribution of WASP-vesicles at the leading edge in cells treated with nocodazole. These results suggest the role of WASP and PCH family proteins not only in the formation of vesicles but possibly in

polarized trafficking of WASP-vesicles to the cortical membrane of the leading and trailing edge, resulting in the polarized F-actin organization during chemotaxis. WASP-vesicles might be associated with MTs temporarily, and MTs facilitate the delivery of these vesicles to the leading edge and the rear by active transport, thereby increasing the probability for a vesicle to encounter a target membrane. There is also a growing evidence for the interplay between the PCH family proteins and microtubules for polarized transport. The polarized secretion of lytic granules by natural killer cells or cytotoxic T lymphocytes is achieved by the polarization of the microtubule organizing centre (MTOC) towards the target and the movement of granules along microtubules in a minus-end direction towards the polarized MTOC[51]. CIP4 has been known to be required for MTOC polarization and cytotoxic activity[52]. Assembly of podosomes in macrophages is dependent on an intact microtubule system and WASP and CIP4 are required for the podosome formation[53]. Some PCH family members contain small GTPase binding (HR1) domains which interact with the Rho GTPases Cdc42, TC10 and Rnd2 [13]. In our previous study, we identified RacC as a major regulator of *Dictyostelium* WASP and a functional orthologue of mammalian Cdc42[54]. It was demonstrated that RacC also localizes on vesicles, suggesting that WASP and RacC might be localized on the same vesicle. Even though it is yet to be determined if NLP or SLP directly interacts with a Rho family GTPase, it is likely that RacC might be involved in the regulation of both NLP/SLP and WASP activity to control vesicle formation and trafficking.

In this study, we demonstrated that roles of NLP/SLP in the formation and microtubule-dependent traffic of WASP-associated vesicles, playing an important role in the spatial regulation of F-actin organization during chemotaxis.

Acknowledgments

We thank Sharon Nelson for excellent technical assistance. We also thank members of the Chung lab for useful discussions and critical reading of the manuscript. We are indebted to Dr. Gunter Gerisch for the golvesin-c-GFP construct, Dr. Angelika Noegel for comitin and interaptin antibodies, and Dr. Thierry Soldati for GFP-HDEL construct. This work was supported, in part, by a grant from National Institute of Health (GM68097 to C.Y.C.).

References

1. Locker J, Goldblatt PJ, Leighton J. Ultrastructural features of invasion in chick embryo liver metastasis of Yoshida ascites hepatoma. Cancer Res 1970;30:1632–1644. [PubMed: 4318696]
2. Lahrtz F, Piali L, Spanaus KS, Seebach J, Fontana A. Chemokines and chemotaxis of leukocytes in infectious meningitis. J Neuroimmunol 1998;85:33–43. [PubMed: 9626995]
3. Downey GP. Mechanisms of leukocyte motility and chemotaxis. Curr Opin Immunol 1994;6:113–124. [PubMed: 8172673]
4. Devreotes PN, Zigmond SH. Chemotaxis in eukaryotic cells: A focus on leukocytes and Dictyostelium. Annu Rev Cell Biol 1988;4:649–686. [PubMed: 2848555]
5. Symons M, Derry JM, Karlak B, Jiang S, Lemahieu V, Mccormick F, Francke U, Abo A. Wiskott-Aldrich syndrome protein, a novel effector for the GTPase CDC42Hs, is implicated in actin polymerization. Cell 1996;84:723–734. [PubMed: 8625410]
6. Zigmond SH. How WASP regulates actin polymerization. J Cell Biol 2000;150:F117–120. [PubMed: 10995455]
7. Aspenstrom P. A Cdc42 target protein with homology to the non-kinase domain of FER has a potential role in regulating the actin cytoskeleton. Current Biology 1997;7:479–487. [PubMed: 9210375]
8. John Lippincott RL. Involvement of PCH family proteins in cytokinesis and actin distribution. Microscopy Research and Technique 2000;49:168–172. [PubMed: 10816256]
9. Dawson JC, Legg JA, Machesky LM. Bar domain proteins: a role in tubulation, scission and actin assembly in clathrin-mediated endocytosis. Trends in Cell Biology 2006;16:493–498. [PubMed: 16949824]

10. Itoh T, Erdmann KS, Roux A, Habermann B, Werner H, De Camilli P. Dynamin and the Actin Cytoskeleton Cooperatively Regulate Plasma Membrane Invagination by BAR and F-BAR Proteins. Developmental Cell 2005;9:791–804. [PubMed: 16326391]
11. Heath RJW, Insall RH. F-BAR domains: multifunctional regulators of membrane curvature. J Cell Sci 2008;121:1951–1954. [PubMed: 18525024]
12. Tsujita K, Suetsugu S, Sasaki N, Furutani M, Oikawa T, Takenawa T. Coordination between the actin cytoskeleton and membrane deformation by a novel membrane tubulation domain of PCH proteins is involved in endocytosis. J Cell Biol 2006;172:269–279. [PubMed: 16418535]
13. Chitu V, Stanley ER. Pombe Cdc15 homology (PCH) proteins: coordinators of membrane-cytoskeletal interactions. Trends Cell Biol 2007;17:145–156. [PubMed: 17296299]
14. Kessels MM, Dong J, Leibig W, Westermann P, Qualmann B. Complexes of syndapin II with dynamin II promote vesicle formation at the trans-Golgi network. J Cell Sci 2006;119:1504–1516. [PubMed: 16551695]
15. Itoh T, De Camilli P. BAR, F-BAR (EFC) and ENTH/ANTH domains in the regulation of membrane-cytosol interfaces and membrane curvature. Biochimica et Biophysica Acta (BBA) - Molecular and Cell Biology of Lipids 2006;1761:897–912.
16. Qualmann B, Kelly RB. Syndapin Isoforms Participate in Receptor-mediated Endocytosis and Actin Organization. J Cell Biol 2000;148:1047–1062. [PubMed: 10704453]
17. Chitu V, Pixley FJ, Macaluso F, Larson DR, Condeelis J, Yeung YG, Stanley ER. The PCH Family Member MAYP/PSTPIP2 Directly Regulates F-Actin Bundling and Enhances Filopodia Formation and Motility in Macrophages. Mol Biol Cell 2005;16:2947–2959. [PubMed: 15788569]
18. Myers SA, Han JW, Lee Y, Firtel RA, Chung CY. A Dictyostelium homologue of WASP is required for polarized F-actin assembly during chemotaxis. Mol Biol Cell 2005;16:2191–2206. [PubMed: 15728724]
19. Chung CY, Firtel RA. PAKa, a putative PAK family member, is required for cytokinesis and the regulation of the cytoskeleton in Dictyostelium discoideum cells during chemotaxis. J Cell Biol 1999;147:559–575. [PubMed: 10545500]
20. Zigmond SH, Joyce M, Borleis J, Bokoch GM, Devreotes PN. Regulation of actin polymerization in cell-free systems by GTPgammaS and Cdc42. J Cell Biol 1997;138:363–374. [PubMed: 9230078]
21. Weiner OH, Murphy J, Griffiths G, Schleicher M, Noegel AA. The actin-binding protein comitin (p24) is a component of the Golgi apparatus. J Cell Biol 1993;123:23–34. [PubMed: 8408201]
22. Monnat J, Neuhaus EM, Pop MS, Ferrari DM, Kramer B, Soldati T. Identification of a Novel Saturable Endoplasmic Reticulum Localization Mechanism Mediated by the C-Terminus of a Dictyostelium Protein Disulfide Isomerase. Mol Biol Cell 2000;11:3469–3484. [PubMed: 11029049]
23. Schneider N, Schwartz JM, Kohler J, Becker M, Schwarz H, Gerisch G. Golvesin-GFP fusions as distinct markers for Golgi and post-Golgi vesicles in Dictyostelium cells. Biol Cell 2000;92:495–511. [PubMed: 11229601]
24. Badour K, Zhang J, Shi F, McGavin MKH, Rampersad V, Hardy LA, Field D, Siminovitch KA. The Wiskott-Aldrich Syndrome Protein Acts Downstream of CD2 and the CD2AP and PSTPIP1 Adaptors to Promote Formation of the Immunological Synapse. Immunity 2003;18:141–154. [PubMed: 12530983]
25. Heath RJW, Insall RH. Dictyostelium MEGAPs: F-BAR domain proteins that regulate motility and membrane tubulation in contractile vacuoles. J Cell Sci 2008;121:1054–1064. [PubMed: 18334553]
26. Kamioka Y, Fukuhara S, Sawa H, Nagashima K, Masuda M, Matsuda M, Mochizuki N. A Novel Dynamin-associating Molecule, Formin-binding Protein 17, Induces Tubular Membrane Invaginations and Participates in Endocytosis. J Biol Chem 2004;279:40091–40099. [PubMed: 15252009]
27. Kessels MM, Qualmann B. Syndapins integrate N-WASP in receptor-mediated endocytosis. EMBO J 2002;21:6083–6094. [PubMed: 12426380]
28. Merrifield CJ, Feldman ME, Wan L, Almers W. Imaging actin and dynamin recruitment during invagination of single clathrin-coated pits. Nat Cell Biol 2002;4:691–698. [PubMed: 12198492]
29. Xu H, Shields D. Prohormone processing in the trans-Golgi network: endoproteolytic cleavage of prosomatostatin and formation of nascent secretory vesicles in permeabilized cells. J Cell Biol 1993;122:1169–1184. [PubMed: 8104189]

30. Ling WL, Shields D. Formation of secretory vesicles in permeabilized cells: a salt extract from yeast membranes promotes budding of nascent secretory vesicles from the trans-Golgi network of endocrine cells. Biochem J 1996;314:723–726. [PubMed: 8615761]
31. Deretic D, Puleo-Scheppke B, Trippe C. Cytoplasmic Domain of Rhodopsin Is Essential for Post-Golgi Vesicle Formation in a Retinal Cell-free System. J Biol Chem 1996;271:2279–2286. [PubMed: 8567690]
32. Westphal M, Jungbluth A, Heidecker M, Muhlbauer B, Heizer C, Schwartz JM, Marriott G, Gerisch G. Microfilament dynamics during cell movement and chemotaxis monitored using a GFP-actin fusion protein. Curr Biol 1997;7:176–183. [PubMed: 9276758]
33. Gerisch G, Albrecht R, Heizer C, Hodgkinson S, Maniak M. Chemoattractant-controlled accumulation of coronin at the leading edge of Dictyostelium cells monitored using green fluorescent protein-coronin fusion protein. Curr Biol 1995;5:1280–1285. [PubMed: 8574585]
34. Firtel RA, Chung CY. The molecular genetics of chemotaxis: sensing and responding to chemoattractant gradients. BioEssays 2000;22:603–615. [PubMed: 10878573]
35. Hall, AL. The regulation of actin polymerization during amoeboid chemotaxis in Dictyostelium discoideum. Yeshiva University; New York, NY: 1989. p. 233
36. Tian L, Nelson DL, Stewart DM. Cdc42-interacting Protein 4 Mediates Binding of the Wiskott-Aldrich Syndrome Protein to Microtubules. J Biol Chem 2000;275:7854–7861. [PubMed: 10713100]
37. Linder S, Hufner K, Wintergerst U, Aepfelbacher M. Microtubule-dependent formation of podosomal adhesion structures in primary human macrophages. J Cell Sci 2000;113:4165–4176. [PubMed: 11069762]
38. Fujita H, Katoh H, Ishikawa Y, Mori K, Negishi M. Rapostlin Is a Novel Effector of Rnd2 GTPase Inducing Neurite Branching. J Biol Chem 2002;277:45428–45434. [PubMed: 12244061]
39. Chung CY, Funamoto S, Firtel RA. Signaling pathways controlling cell polarity and chemotaxis. TIBS 2001;26:557–566. [PubMed: 11551793]
40. Qualmann B, Mellor H. Regulation of endocytic traffic by Rho GTPases. Biochem J 2003;371:233–241. [PubMed: 12564953]
41. Ridley AJ. Rho GTPases and actin dynamics in membrane protrusions and vesicle trafficking. Trends Cell Biol 2006;16:522–529. [PubMed: 16949823]
42. Traynor D, Kay RR. Possible roles of the endocytic cycle in cell motility. J Cell Sci 2007;120:2318–2327. [PubMed: 17606987]
43. Lázaro-Diégueza F, Colonnaa C, Corteganoa M, Calvod M, Martíneza SE, Egea G. Variable actin dynamics requirement for the exit of different cargo from the trans-Golgi network. FEBS letters 2007;581:3875–3881. [PubMed: 17651738]
44. Rozelle A, Machesky L, Yamamoto M, Driessens M, Insall R, Roth M, Luby-Phelps M, Marriott G, Hall AH. Phosphatidylinositol 4,5-bisphosphate induces actin-based movement of raft-enriched vesicles through WASP-Arp2/3. Curr Biol 2000;10:311–320. [PubMed: 10744973]
45. Percival JM, Hughes JA, Brown DL, Schevzov G, Heimann K, Vrhovski B, Bryce N, Stow JL, Gunning PW. Targeting of a tropomyosin isoform to short microfilaments associated with the Golgi complex. Mol Biol Cell 2004;15:268–280. [PubMed: 14528022]
46. Taunton J, Rowning BA, Coughlin ML, Wu M, Moon RT, Mitchison TJ, Larabell CA. Actin-dependent propulsion of endosomes and lysosomes by recruitment of N-WASP. J Cell Biol 2000;148:519–530. [PubMed: 10662777]
47. Carreno S, Engqvist-Goldstein AE, Zhang CX, McDonald KL, Drubin DG. Actin dynamics coupled to clathrin-coated vesicle formation at the trans-Golgi network. J Cell Biol 2004;165:781–788. [PubMed: 15210728]
48. Higgs HN, Pollard TD. Activation by Cdc42 and PIP(2) of Wiskott-Aldrich syndrome protein (WASp) stimulates actin nucleation by Arp2/3 complex. J Cell Biol 2000;150:1311–1320. [PubMed: 10995437]
49. Rohatgi R, Ho HY, Kirschner MW. Mechanism of N-WASP activation by CDC42 and phosphatidylinositol 4, 5-bisphosphate. J Cell Biol 2000;150:1299–1310. [PubMed: 10995436]
50. Shimada A, Niwa H, Tsujita K, Suetsugu S, Nitta K, Hanawa-Suetsugu K, Akasaka R, Nishino Y, Toyama M, Chen L, Liu ZJ, Wang BC, Yamamoto M, Terada T, Miyazawa A, Tanaka A, Sugano S, Shirouzu M, Nagayama K, Takenawa T, Yokoyama S. Curved EFC/F-BAR-domain dimers are

joined end to end into a filament for membrane invagination in endocytosis. Cell 2007;129:761–772. [PubMed: 17512409]

51. Stinchcombe JC, Majorovits E, Bossi G, Fuller S, Griffiths GM. Centrosome polarization delivers secretory granules to the immunological synapse. Nature 2006;443:462–465. [PubMed: 17006514]
52. Banerjee PP, Pandey R, Zheng R, Suhoski MM, Monaco-Shawver L, Orange JS. Cdc42-interacting protein-4 functionally links actin and microtubule networks at the cytolytic NK cell immunological synapse. J Exp Med 2007;204:2305–2320. [PubMed: 17785506]
53. Linder S, Higgs H, Hufner K, Schwarz K, Pannicke U, Aepfelbacher M. The polarization defect of Wiskott-Aldrich syndrome macrophages is linked to dislocalization of the Arp2/3 complex. J Immunol 2000;165:221–225. [PubMed: 10861055]
54. Han JW, Leeper L, Rivero F, Chung CY. Role of RacC for the regulation of wasp and phosphatidylinositol 3-kinase during chemotaxis of Dictyostelium. J Biol Chem 2006;281:35224–35234. [PubMed: 16968699]

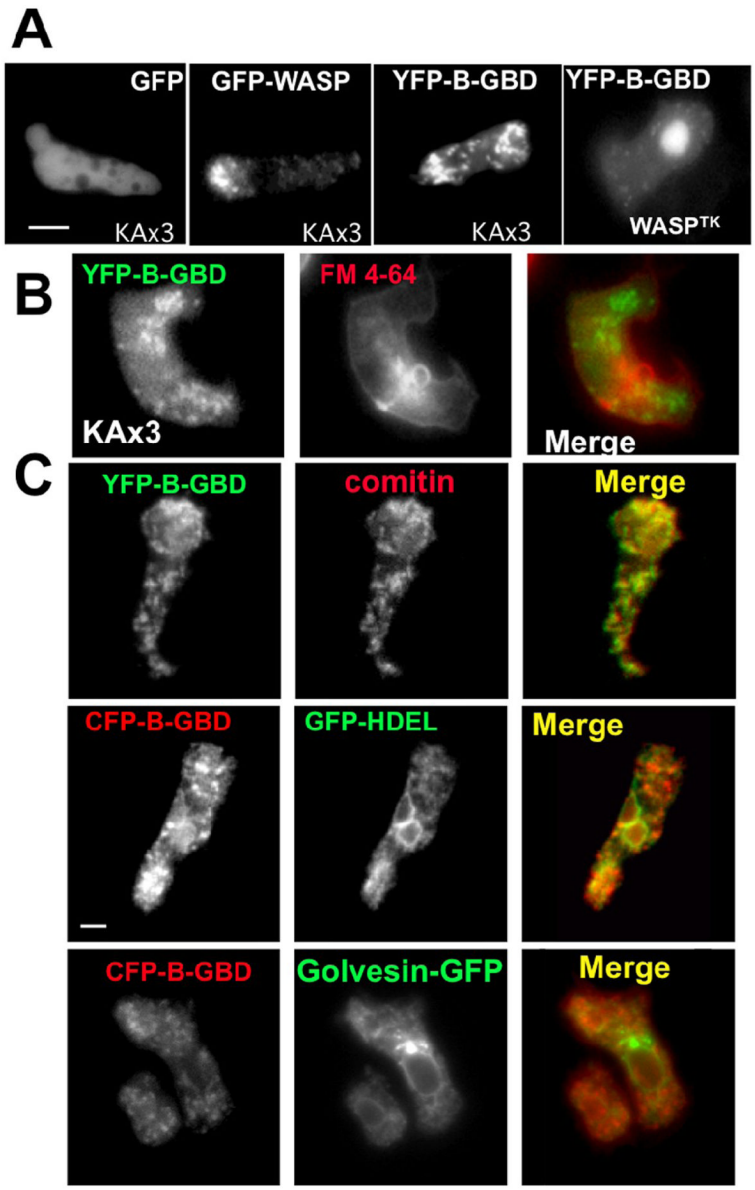

Figure 1.

(A) Localization of GFP-WASP or YFP-B-GBD expressed in *Dictyostelium* cells migrating toward a cAMP gradient. Cells were pulsed for 5 hours and localizations of GFP-WASP or YFP-B-GBD in aggregation-competent KAx3 cells, or YFP-B-GBD in $WASP^{TK}$ cells were examined. Bar = 5 μm. (B) KAx3 cells were stained with FM4-64, a marker for internalized endosomal compartments, for 2 min and washed. After 10 min delay, cells were imaged to determine the colocalization. (C) KAx3 cells expressing YFP-B-GBD were stained with an antibody against comitin (a marker for Golgi and Golgi-derived cesicles). In bottom panels, fluorescence images of living cells co-expressing GFP-HDEL(an ER-specific retrieval signal in *Dictyostelium*) or golvesin-c-GFP (a marker for Golgi but not for Golgi-derived vesicles) and CFP-B-GBD are shown. Bar = 5 μm.

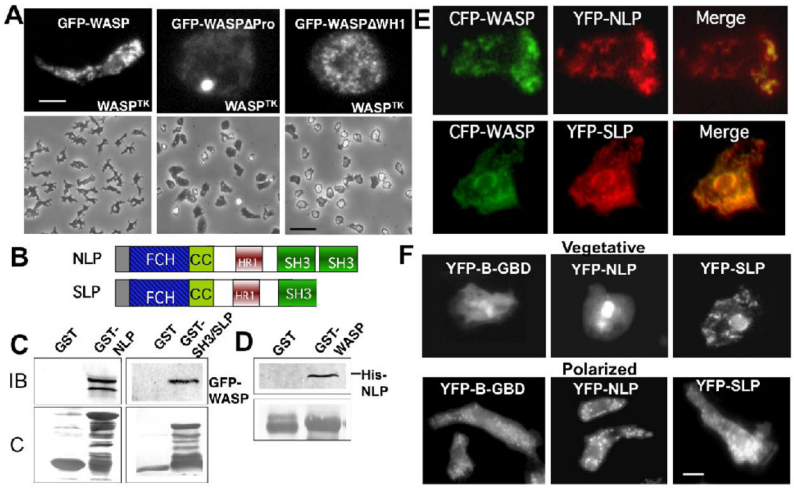

Figure 2.

(A) Top panels show localization of GFP-WASP, GFP-WASPΔPro and GFP-WASPΔWH1 expressed in $WASP^{TK}$ cells (bar = 5 μm). Bottom panels show phase contrast pictures of these cells at lower magnification (bar = 50 μm). (B) Schematic diagram of NLP/SLP domain structure. FCH: FER/CIP4-homology; CC: coiled-coil; HR1: homology region 1; SH3: Src homology 3. (C) GST pull-down assay showing the interaction between WASP and NLP/SLP. GST-NLP- or GST-SH3 (SH3 domain of SLP)-bound agarose beads were incubated with the lysate of GFP-WASP expressing cells. Bound GFP-WASP was detected by immunoblot with the anti-GFP antibody. IB: immunoblot; C: Coomassie Blue staining. (D) Direct interaction between purified 6X His-tagged NLP and GST-WASP was also confirmed by pull down assay. (E) Fluorescence images of aggregation-competent cells co-expressing CFP-WASP and YFP-NLP or -SLP are shown. CFP-WASP showed punctate vesicle labeling which appears to overlap with YFP-NLP or 2 signal and these vesicles were enriched at the leading edge of migrating cells. (F) Change of subcellular localization of NLP/SLP upon polarization of cells. Images of YFP-NLP, YFP-SLP, or YFP-B-GBD were taken in cells at growth stage and in polarized cells at aggregation-competent stage. NLP/SLP are localized at the perinuclear region in non-polarized cells at growth stage, but with vesicles in polarized cells.

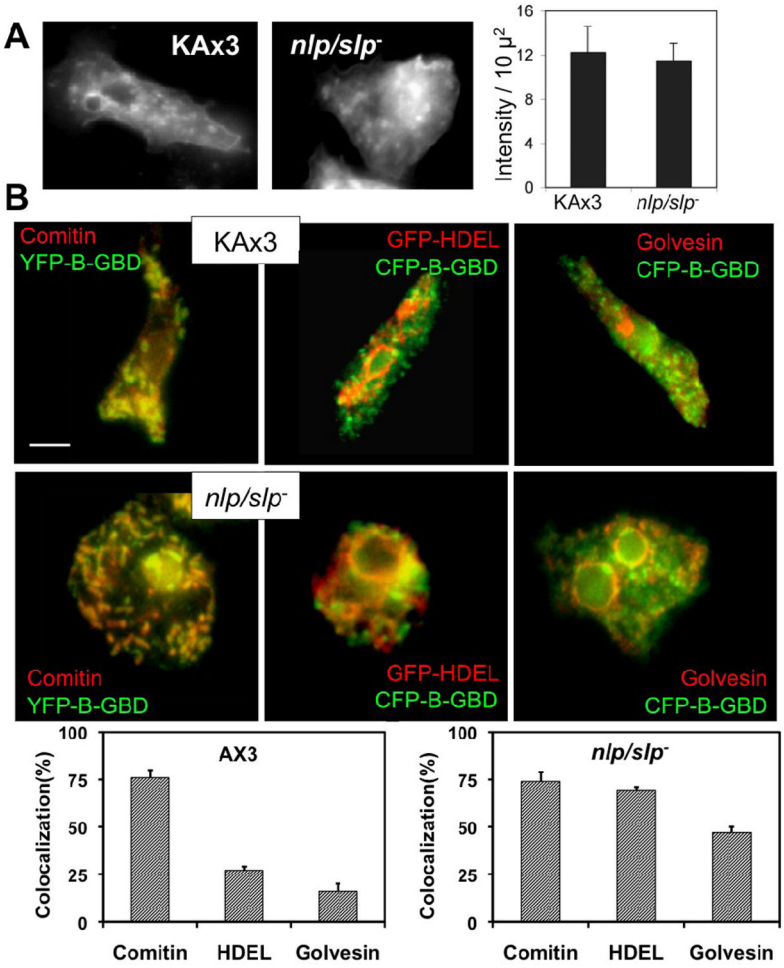

Figure 3.

(A) Membrane endocytosis by aggregation-competent cells determined using FM1-43X. Ax3 or *nlp/slp*- cells were incubated with FM1-43X for 2 min and washed, followed by fixation for image collection. Cells were fixed after 2 min incubation with FM 1-43 followed by a 10 min delay to allow for endocytosis. Fluorescence intensity of FM1-43X dye in cells was measured and shown in the graph. Error bars represent SEM (n=10). (B) Colocalization of CFP-B-GBD with GFP-HDEL and golvesin-c-GFP in *nlp/slp*- cells. GFP-HDEL and golvesin-c-GFP overlaps with CFP-B-GBD in *nlp/slp*- cells, but not in KAx3 cells. At least 15 cells from two independent experiments were analyzed for colocalization as decribed in Methods section. The percent colocalization calculated among areas is shown for the percentage of YFP-B-GBD that colocalized with comitin, GFP-HDEL, or golvesin-c-GFP respectively.

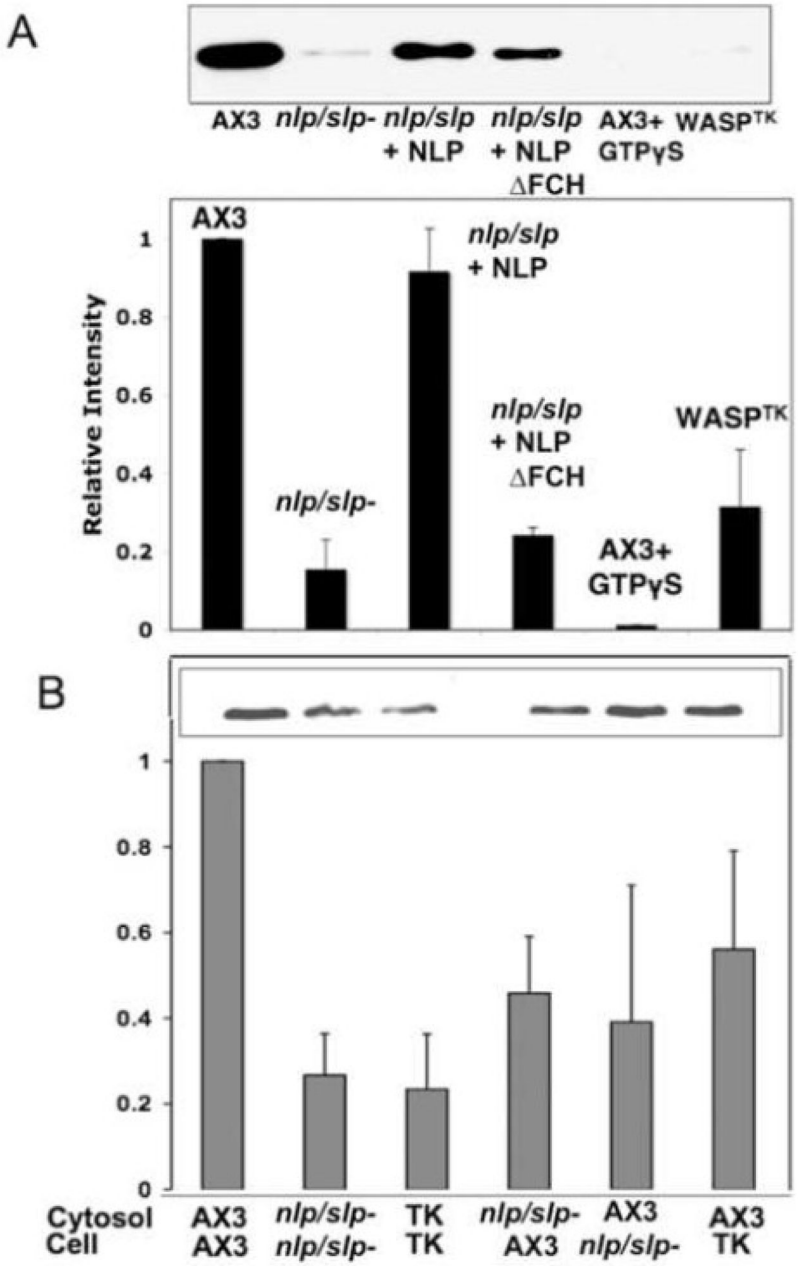

Figure 4.

Vesicle formation reconstitution assay. The role of NLP/SLP for vesicle formation from Golgi was examined using an assay that reconstitutes the formation of vesicles in a cell-free system. (A) Immunoblot of comitin on secretory vesicles formed in permeabilized cells reconstituted with the cytosol fraction prepared from the cell lysate. *nlp/slp*$^{-}$ and WASP^{TK} cells showed significantly reduced formation of vesicles, which can be rescued by GST-NLP, but not with NLP lacking FCH domain. Graph shows quantification of band intensities from four separate immunoblots. (B) Vesicle formation was measured in different combinations of the cytosols and permeabilized cells of wild type, *nlp/slp-*, or WASP^{TK} cells.

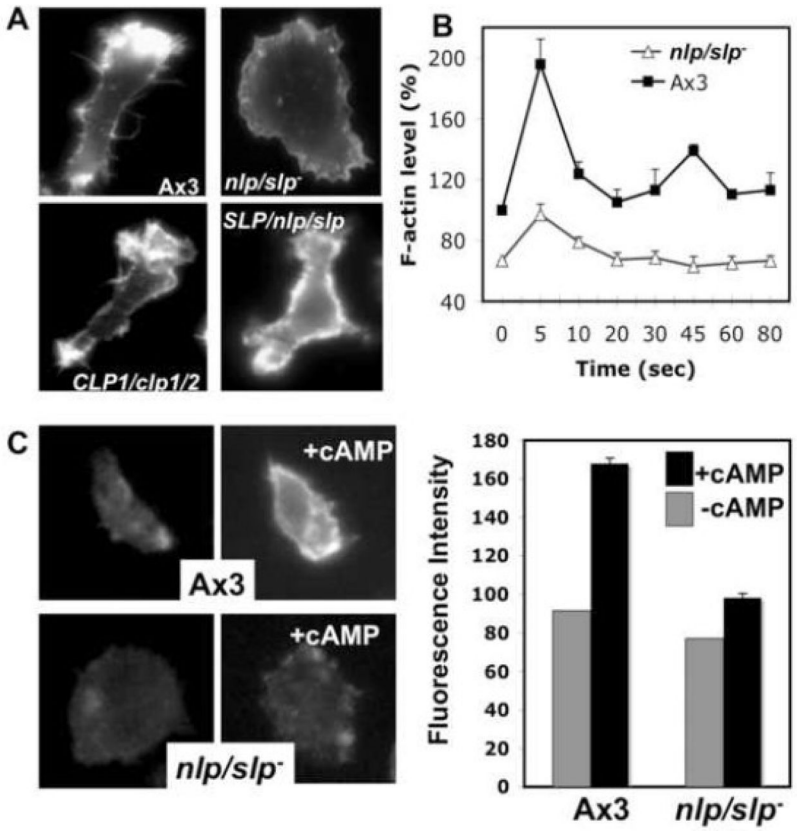

Figure 5.

F-actin organization and chemotaxis of *nlp/slp*- cells. (A) Aggregation-competent cells were fixed and stained with phallioidin. *nlp/slp*- cells exhibited severe defects in F-actin organization as they exhibit neither a prominent F-actin-enriched lamellipod nor cell polarity. This defect can be rescued by the expression of NLP or SLP. (B) *In vivo* actin polymerization assay measuring F-actin assembled in response to the chemoattractant (cAMP) stimulation. Basal F-actin level before cAMP stimulation is lower in *nlp/slp*- cells and F-actin polymerization upon cAMP stimulation is also defective in *nlp/slp*- cells. Error bars represent SEM (n=4) (C) Barbed-end staining of KAx3 or *nlp/slp*- cells. Barbed-ends were stained with Alexa595-labeled G-actin before and 5 seconds after cAMP stimulation. *nlp/slp*- cells show a greatly decreased number of free barbed ends at the cortical membrane upon cAMP stimulation relative to wild-type cells. A linescan analysis was performed to measure the pixel intensity at cortical membrane after background subtraction. Average fluorescence intensities measured at the cortical membrane (4 linescans per cell and 10–12 cells total) before and after cAMP stimulation are presented in the graph. Error bars represent SEM (n=8)

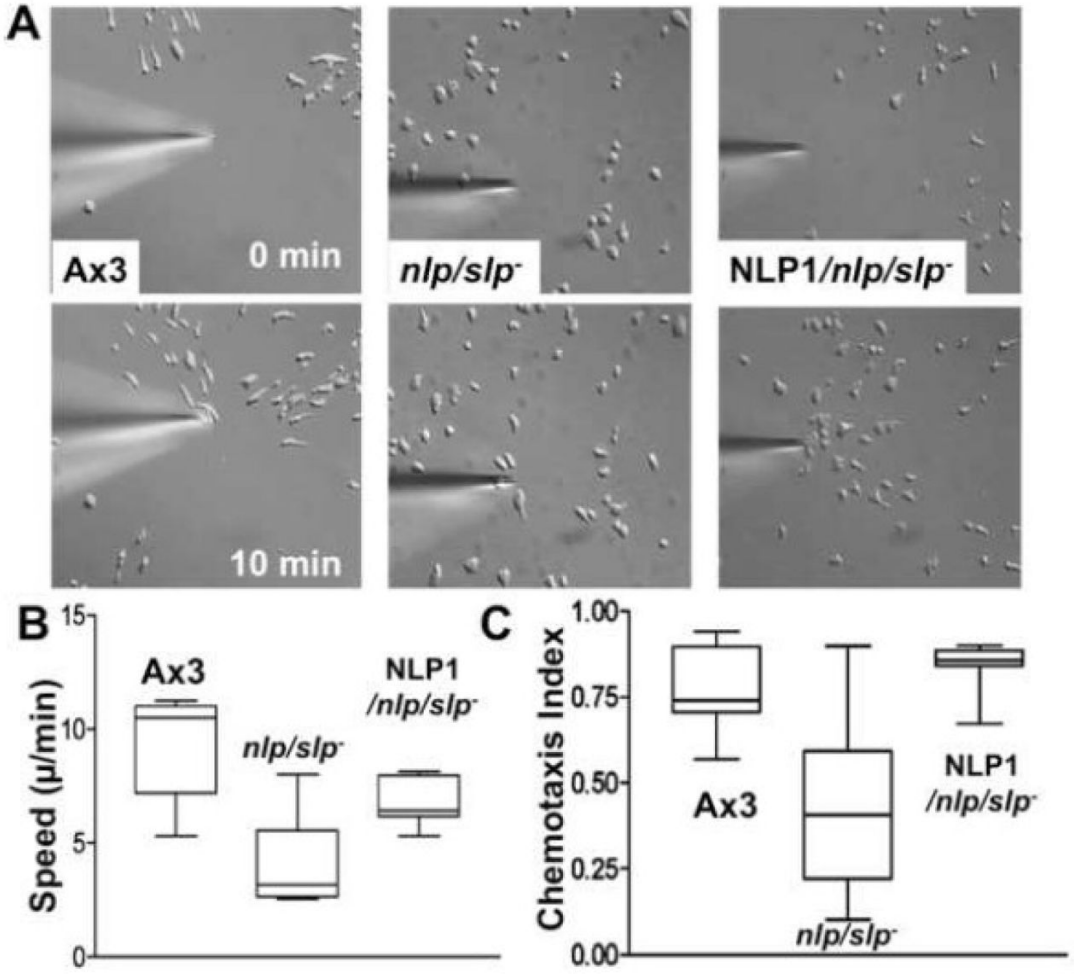

Figure 6.

Abnormal chemotactic movement of *nlp/slp-* cells. (A) DIC images of cells migrating toward a cAMP gradient at 0 or 10 min. Wild-type cells are usually well polarized, move quickly and linearly toward the cAMP source. *nlp/slp-* cells appear to have difficulties developing a psuedopod in the direction of the chemoattractant gradient. The expression of YFP-NLP alone mostly rescues motility defects. (B) The speed and chemotaxis index of *nlp/slp-* cells is significantly decreased compared to KAx3 cells, but recovered by the expression of NLP. Chemotaxis of at least 7 cells from two independent experiments was measured.

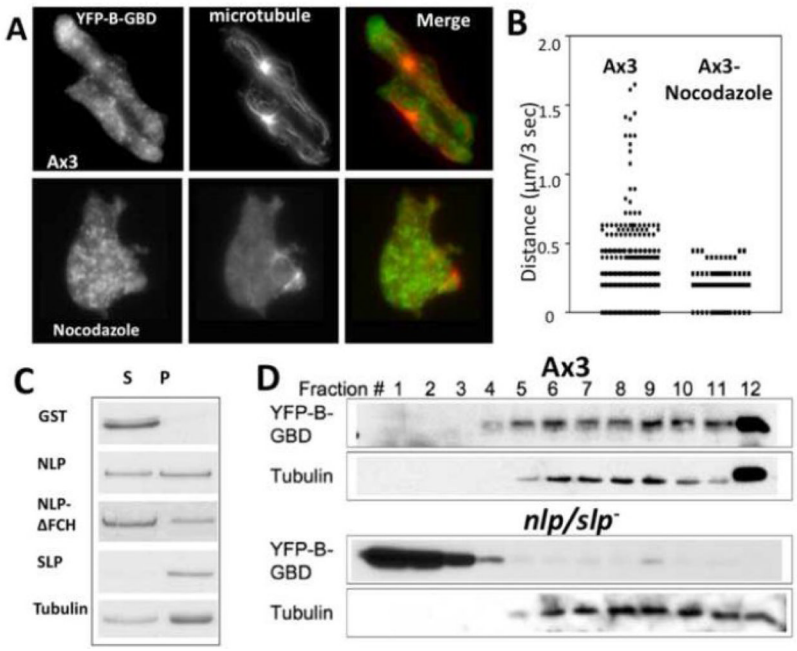

Figure 7.

(A) Distribution of vesicles decorated with YFP-B-GBD in chemotaxing or nocodazole-treated cells. Cells expressing YFP-B-GBD in aggregation stage were fixed and stained with rabbit anti-tubulin antibody. The YFP-B-GBD and microtubule images were superimposed for assessment of localization of YFP-B-GBD vesicles in a close proximity to microtubules. (B) Tracking of YFP-B-GBD vesicle movements in KAx3 or nocodazole-treated cells by live cell imaging. Speed of vesicle movement in wild type or cells treated with nocodazole was measured and plotted. Wild type cells showed brief periods of rapid directed movement leading to high speed (>0.25 μm/sec) that is absent in nocodazole-treated cells. (C) Binding of NLP/SLP and a NLP mutant to microtubule. GST-NLP or SLP were incubated with paclitaxel stabilized-microtubules. Supernatants (s) and pellets (p) were collected after ultracentrifugation over a 15% sucrose cushion and analyzed by SDS-PAGE for presence of GST-NLP or SLP by SDS-PAGE. (D) Cosedimentation of YFP-B-GBD with MT on a sucrose gradient. Lysates of wild type or *nlp/slp*- cells expressing YFP-B-GBD were applied onto 15–40% sucrose gradient and fractions were collected. YFP-B-GBD in fractions was detected by western blot with anti-GFP antibody.